nature materials

REVIEW ARTICLE

PUBLISHED ONLINE: 22 OCTOBER 2015 | DOI: 10.1038/NMAT4433

Programmable and adaptive mechanics with liquid crystal polymer networks and elastomers

Timothy J. White[1]* and Dirk J. Broer[2]*

Liquid crystals are the basis of a pervasive technology of the modern era. Yet, as the display market becomes commoditized, researchers in industry, government and academia are increasingly examining liquid crystalline materials in a variety of polymeric forms and discovering their fascinating and useful properties. In this Review, we detail the historical development of liquid crystalline polymeric materials, with emphasis on the thermally and photogenerated macroscale mechanical responses — such as bending, twisting and buckling — and on local-feature development (primarily related to topographical control). Within this framework, we elucidate the benefits of liquid crystallinity and contrast them with other stimuli-induced mechanical responses reported for other materials. We end with an outlook of existing challenges and near-term application opportunities.

Liquid crystals (LCs) were identified as a state of matter near the end of the nineteenth century[1], and have since then remained a topic of intense scientific curiosity. LCs self-organize at the molecular level (Box 1), and are classified into the subcategories of thermotropic (order depends on temperature), lyotropic (order depends on the concentration of material in solution) and phototropic (order depends on the presence of light)[2,3]. Spurred by the employment of low-molar-mass LCs in display technologies, research of these materials has rapidly grown in recent decades, and is now extending into areas beyond displays, including solar-energy harvesting[4,5], optics and photonics[6], mechanics[7] and biomedicine[8].

Polymeric materials exhibiting liquid crystallinity have been referred to by a variety of names, including liquid crystal polymers (LCPs), polymeric LCs, liquid crystal elastomers (LCEs), and liquid crystal polymer networks (LCNs). The differences in the chemical composition, crosslinking and thermomechanical properties of these materials are illustrated in Fig. 1. A liquid crystal main-chain polymer (LCP; Fig. 1a) is a high-performance and typically uncrosslinked macromolecule (such as Vectran) that can organize into liquid crystalline phases through stiff rod-like molecular conformation and intramolecular interactions (most commonly, hydrogen bonding). LCNs (Fig. 1b) maintain some of the high-performance properties of LCPs, but notably contain a moderate to densely crosslinked network architecture associated with their preparation from primarily (meth)acrylate-based multifunctional monomers. Whereas LCPs exhibit almost no change in order (described by the order parameter, S), the order of LCNs can decrease by as much as 5% when subjected to appropriate stimuli. LCEs (Fig. 1c) also consist of crosslinked liquid-crystal side-chain and/or main-chain mesogenic units[9,10], but the polymer backbone is typically flexible (commonly a polysiloxane) and the overall crosslink density is low. Unlike LCPs or LCNs, LCEs can exhibit large changes in order when subject to a stimulus. Swelling both LCNs or LCEs to form liquid crystalline gels (LCGs) can further sensitize the response of the polymeric materials to stimuli[11], most notably to electric fields[12,13].

In this Review, we discuss the remarkable properties of LCNs and LCEs, and focus specifically on the burgeoning area of stimuli-initiated actuation and shape change. We start by briefly introducing how these materials are prepared before discussing the response of LCNs and LCEs to temperature. We then review recent results on the response of these materials to heat, light and magnetic fields. Notably, we highlight efforts on the programming of LCN and LCE materials to localize their mechanical response so as to generate surface features or shape change. We close with a forward-looking overview of the implications of these materials for a range of applications.

Preparation and properties of LCEs and LCNs

The preparation of polymeric materials that exhibit liquid crystallinity was initially pursued by Vorländer[14], and first realized by Jackson and Kuhfuss[15]. Concurrent to advances in the development and application of low-molar-mass LCs in display applications, researchers achieved the preparation of well-ordered LCEs by crosslinking side-chain polymers[16–19], where the mesogenic groups are attached to siloxane or acrylate polymer main chains (Fig. 2a). A two-step crosslinking technique was developed in which the pendant mesogenic groups were oriented by mechanical stretching of the polymer during or shortly after the first-stage reaction, after which the alignment is fixed by a second-stage crosslinking reaction to form highly aligned LCEs (so-called single-crystal or monodomain LCEs). The molecular structure of a LCE corresponds to that of a traditional rubber: it consists of long chains of molecules that can easily slip past one another and thus enable the material to be expanded with very little force. Attached to the elastomer chains are the smaller rod-like molecular entities similar to those usually found in low-molar-mass LC molecules. The weak crosslinking in the LCE allows spontaneous shape changes (strains) of several hundred per cent (Fig. 2b,c) under load, and by the application of stress or strain they can exhibit some unusual mechano-optical effects[20]. The mechanical responses depend on the direction of the applied stress relative to the material's alignment direction and its phase (smectic, nematic, cholesteric or isotropic). The stress–strain response of these materials has been described as 'soft elasticity' (Fig. 2d), a term that refers to the strain that these materials exhibit at near-zero stress while the director is reorienting to the strain direction (the physics of this process has been described in detail in ref. 21). The optical properties of LCEs are comparable to

[1]Air Force Research Laboratory, Materials and Manufacturing Directorate, Wright-Patterson Air Force Base, Ohio 45433, USA. [2]Eindhoven University of Technology, Institute for Complex Molecular Systems, Department of Chemical Engineering and Chemistry, Helix Building STO 0.34, PO Box 513, 5600 MB Eindhoven, The Netherlands. *e-mail: timothy.white.24@us.af.mil; d.broer@tue.nl

Box 1 | Order and orientation of liquid crystals.

The term 'liquid crystal' refers to materials that exhibit long-range orientational or positional organization at the molecular level. In low-molar-mass LCs of the calamitic subclass (the basis of displays), the molecules self-organize to form a variety of mesophases, including nematic or chiral nematic (one dimension of order, in this case orientational), numerous variants of smectic (two dimensions of order, orientational and positional), and more complex geometries, such as those of the blue or bent-core phases. The order of low-molar-mass LCs can be affected by temperature or light, which can result in transitions between these phases or to an isotropic state.

Similarly, in polymeric variants, the term 'liquid crystalline' indicates that the material has either orientational or positional order of mesogenic units in the polymer backbone (main chain) or pendant groups (side chain). Figure 1 illustrates select chemical structures of different subsets of liquid crystalline polymers. The sensitivity of the order to stimuli is strongly dependent on the composition of the polymer. Inducing chirality through chiral inclusions or surface-alignment treatments generates a hierarchical variation in the profile of the common orientation vector (director) through the sample thickness, as illustrated in Fig. 4a–d.

those of low-molar-mass LCs — a high birefringence and selective reflection of polarized light in the case of the cholesteric phase. Recent examinations of LCEs have demonstrated potential utility as artificial muscles (robotics)[22–26], deformable lasers[27] and sensors[28].

Moderately to densely crosslinked glassy LCNs, which were developed in the 1980s at Philips Research, are obtained from the polymerization of multifunctional mesogenic monomers (Fig. 3a). These monomers exhibit a liquid crystalline phase that can be retained after polymerization (in most cases by photoinitiated polymerization)[29–32]. Copolymerization of monoacrylates, such as RM23, with diacrylates, such as RM82 (Fig. 3a), generate LCNs with side-chain (pendant) and main-chain mesogenic units. The advantages of this approach are numerous. Within reasonable limits, the polymerization temperature can be freely chosen, which enables the desired phase to be retained. Similar to low-molar-mass LCs, the order can be manipulated by external boundary conditions and stimuli (including surface-alignment materials, surfactants, shear forces, and electric, magnetic or optical fields) to prepare engineered materials with complex properties and alignments that are retained indefinitely after polymerization. The ability to arrest the three-dimensional structure of the liquid crystalline phase in polymeric form has created a number of compelling application possibilities (see 'Outlook'). In conventional polymeric materials the methods to produce such structures are limited in number, and no process that we are aware of enables such modularity and programmability. Exhaustive reviews of the materials chemistry and processing methods to prepare LCNs can be found in refs 7, 20 and 28.

Thermomechanical responses

Thermally induced mechanical responses have been widely observed in both LCEs and LCNs[7,20]. These thermomechanical responses are ultimately distinguished from those of other materials by the possibility to programme the material's anisotropy, orientation and alignment to dictate responses that are inherently driven by the heterogeneity in the local orientation of LCN or LCEs rather than by heterogeneities in material composition or sensitivity to stimuli (see 'Outlook').

Loosely crosslinked LCEs exhibit thermotropism, similar to that of low-molar-mass LCs. Accordingly, on heating LCEs through a transition from a liquid crystalline phase (typically nematic) to the isotropic (or paranematic) state, a substantial shrinkage strain is observed parallel to the director vector[10]. The light crosslinking and elastomeric nature of the materials allow for length changes of as much as a factor of four (plotted as L/L_{iso} in Fig. 2c, where L_{iso} is the length in the isotropic state and L the actual length at the measuring temperature in the nematic state). The large macroscopic mechanical response is the result of disorganization of the rod-like mesogenic moieties attached to the polymer main chain and to the coupling of the conformation of the macromolecular backbone with the orientational nematic order S (Fig. 2b)[33,34]. The polymer chains elongate when the mesogens orient in the nematic phase (Fig. 2b), whereas in the isotropic phase they recover, driven by entropy, a random-coil conformation (Fig. 2b). As predicted by de Gennes, the individual polymer-chain shape-changes then translate to a macroscopic shape-change of the elastomer sample at the nematic–isotropic transition[35]. The so-called genesis of the LCE is known to strongly influence the resulting thermomechanical response[36]. These and other theoretical descriptions of contraction and expansion at the nematic-to-isotropic transition stimulated a broader interest in artificial muscles based on thermoresponsive LCEs[10,25,37–39]. Recent work in this topic has focused on exploiting the large, thermally induced mechanical response of LCEs in a variety of applications[40] (see 'Remote heating'). Highlights from the recent literature include the preparation of elastomeric colloidal materials[41,42], the use of LCEs as shape-memory polymers[43–45] and surface-feature patterning[46–49].

The substantial increase in crosslink density in the formation of LCNs from multifunctional liquid-crystalline monomers precludes the material from undergoing thermotropic phase transitions before the decomposition temperature of the materials. LCNs exhibit a glass transition temperature (T_g) that is typically in the range of 40–120 °C (at room temperature, the modulus is in the order of 0.8–2 GPa; ref. 50). Owing to the anisotropy of the system, the compliance of the polymer network perpendicular to the director is roughly three times higher than parallel to it. The mechanical properties of LCNs are strongly influenced by the composition, namely the length of the aliphatic spacer of the crosslinking diacrylate monomer[50,51] (Fig. 3a) and the phase behaviour of the monomer or mixture[31,52,53]. Given the ease of preparation and availability of materials, glassy LCN materials prepared from monomers, such as those illustrated in Fig. 3a, are now widely studied, in particular because of their potential (see 'Outlook').

As with other polymers, the volume of LCNs increases with temperature, and this can be described by the coefficient of thermal expansion α (Fig. 3b). In aligned LCNs, the sign of α is strongly dependent on alignment[52]. Figure 3b illustrates the influence of starting materials and preparation conditions on the thermal expansion of LCN materials. Below T_g, α in the direction parallel to the director is close to zero. Heating above T_g causes α in this axis to become negative. Orthogonal to the director, the thermal expansion rapidly increases above T_g. LCN materials prepared with a longer aliphatic spacer experience a larger volume increase with temperature. Furthermore, the temperature at which the LCN was prepared can also have a profound impact on the thermal response of these materials[52,54]. LCNs prepared close to the nematic-to-isotropic transition (T_p/T_c = 0.96, where T_p and T_c are the polymerization and clearing temperatures, respectively) of the monomer show a smaller response than systems cured further below this LC transition[55] (T_p/T_c = 0.86). A decrease in the curing temperature only slightly affects the order of the polymer network, but leads to a significant increase in the thermomechanical response of the system. For example, for C6M (Fig. 3b), decreasing the T_c from 0.96 to 0.86 increases the order parameter of the network from 0.71 to 0.76, but changes the strain parallel to the director from –1.3% to –1.7% on heating from –50 °C to 150 °C.

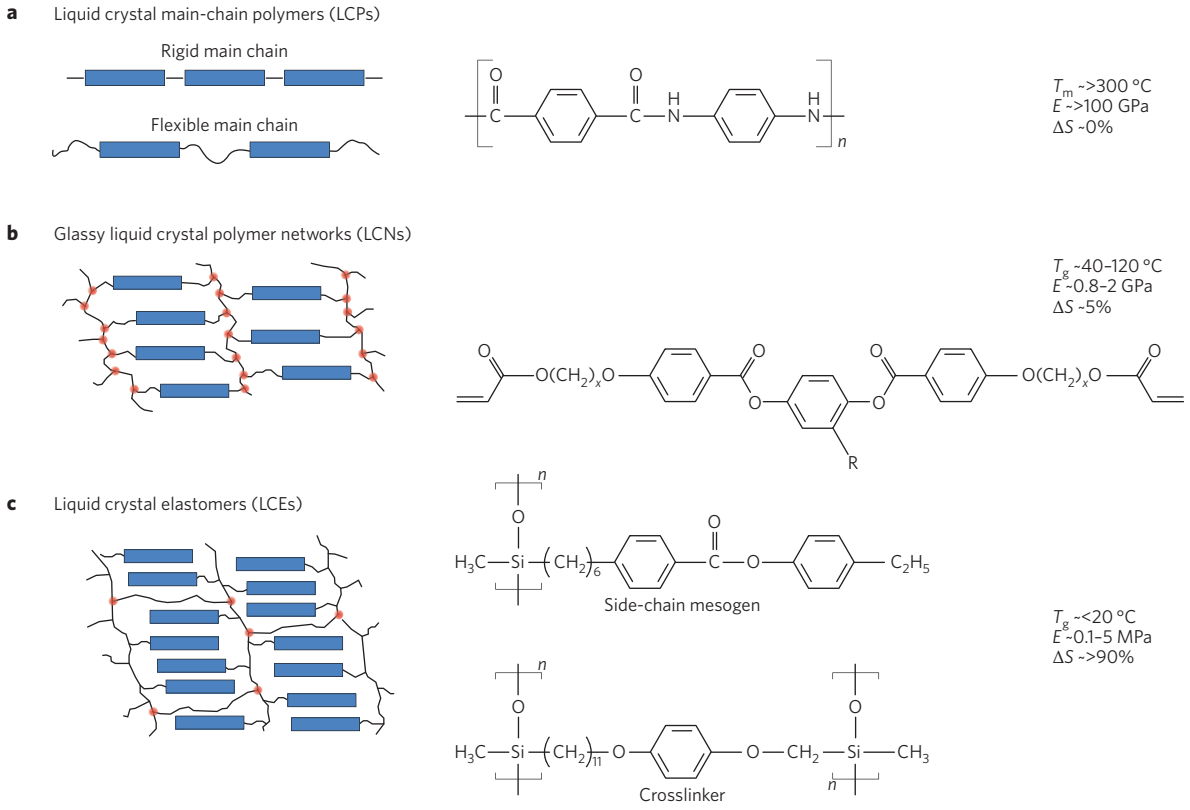

Figure 1 | Liquid crystal polymers, polymer networks and elastomers. a, Liquid crystal polymer (LCP) is a term historically used to refer to high-performance polymeric materials, such as Vectra (chemical structure, right), that form liquid crystalline phases. These materials are typically linear polymers, with melting temperatures (T_m) around or exceeding 300 °C and moduli (E) that can exceed 100 GPa, that undergo minimal change in order (ΔS) on heating. **b**, 'Glassy' liquid crystal polymer networks (LCNs) are moderately to densely crosslinked, and most often formed from the polymerization of mesogenic (meth)acrylate monomers, which yields glassy polymers that can retain distinctive optical or mechanical properties. These materials have glass transition temperatures (T_g) in the interval 40–120 °C and moduli of approximately 1–2 GPa, and on heating can exhibit moderate changes in order. **c**, Liquid crystal elastomers (LCEs) are a subclass of LCNs for which the polymer backbone is commonly polysiloxane and the crosslink density is low. Accordingly, subjecting these materials to appropriate stimuli can generate large changes in the order parameter that yield large strains. Red dots indicate crosslinks, and blue rectangles indicate either main-chain or side-chain mesogenic moieties. Representative chemical formulas are shown (right).

The reduction of order leads to an increasing average tilt of the mesogenic units that decreases the projection of the end-to-end length of the monomeric units. Accordingly, at temperatures below T_g, the system expands with temperature due to increasing molar volume. The preferential expansion direction is perpendicular to the long axis of the molecule, as the expansion is dominated by increasing intramolecular distances. Around and above T_g there is a small and reversible loss of molecular order, which causes additional deformation. The reduction of order is favourable for entropic reasons, but is limited by the polymer network. The measured change in order parameter is small (of the order of a few per cent according to birefringence measurements), yet geometrical arguments show that this change correlates to the mechanical responses evident in Fig. 3b.

In practice, the temperature sensitivity of LCNs and LCEs has been employed to generate shape-adaptive responses. The comparatively limited strain of glassy LCNs has not hindered their examination for potential utility in actuation. Because these films tend to be thin, the temperature distribution across an LCN is uniform. Accordingly, heating LCNs in which the alignment is uniform (Fig. 4a) across the thickness does not induce motion. However, LCNs prepared with hierarchical variation in the director (splay, twisted nematic; Fig. 4c,d) have been shown to bend and coil similarly to a bimetallic strip[55,56]. The thermally induced deflection of hierarchically oriented LCNs is simply related to the anisotropy in α, as is evident in Fig. 3b. As the orientation of the director rotates across the sample thickness, the relative magnitudes of the strain are the same but the orientation of the strain varies, thus resulting in deflection. Further, if the orientation of the LCN is offset to the principal axes of the mechanical specimen, the thermal response can generate shear, yielding helicoidal and spiral ribbons on heating[57–59] (Fig. 4e,f). The generation of a helicoidal or spiral shape is dictated by the aspect ratio of the sample. Moreover, the thermomechanical response can also be harnessed in other geometries[41,60] (fibres, particles) to extend, and in some ways amplify, the nascent thermomechanical response to generate actuation.

Photomechanical effects

A variety of approaches have been used to generate large-scale and efficient transduction of light into work[61–66]. Yet despite considerable effort, the direct conversion of light into large-scale mechanical output (typically measured as strain) was limited to less than 1% in photoresponsive amorphous or semicrystalline polymeric materials[67,68]. In 2001, large-scale optically generated and reversible strain of as much as 20%[69] was achieved in an LCE functionalized with azobenzene (azo-LCE; Fig. 4g). Subsequent examinations have reported increases in strain to 100%, and explored variations to mesogen connectivity[23,70], the inclusion of guest dopants[71], correlations to phototropic phase behaviour[72,73], and theoretical treatments[74–78]. It should be noted that this body of work initiated a renaissance in the pursuit of light-to-work transduction not only in LCEs and LCNs, but also in crystalline solids[79,80] and conventional polymeric materials[66].

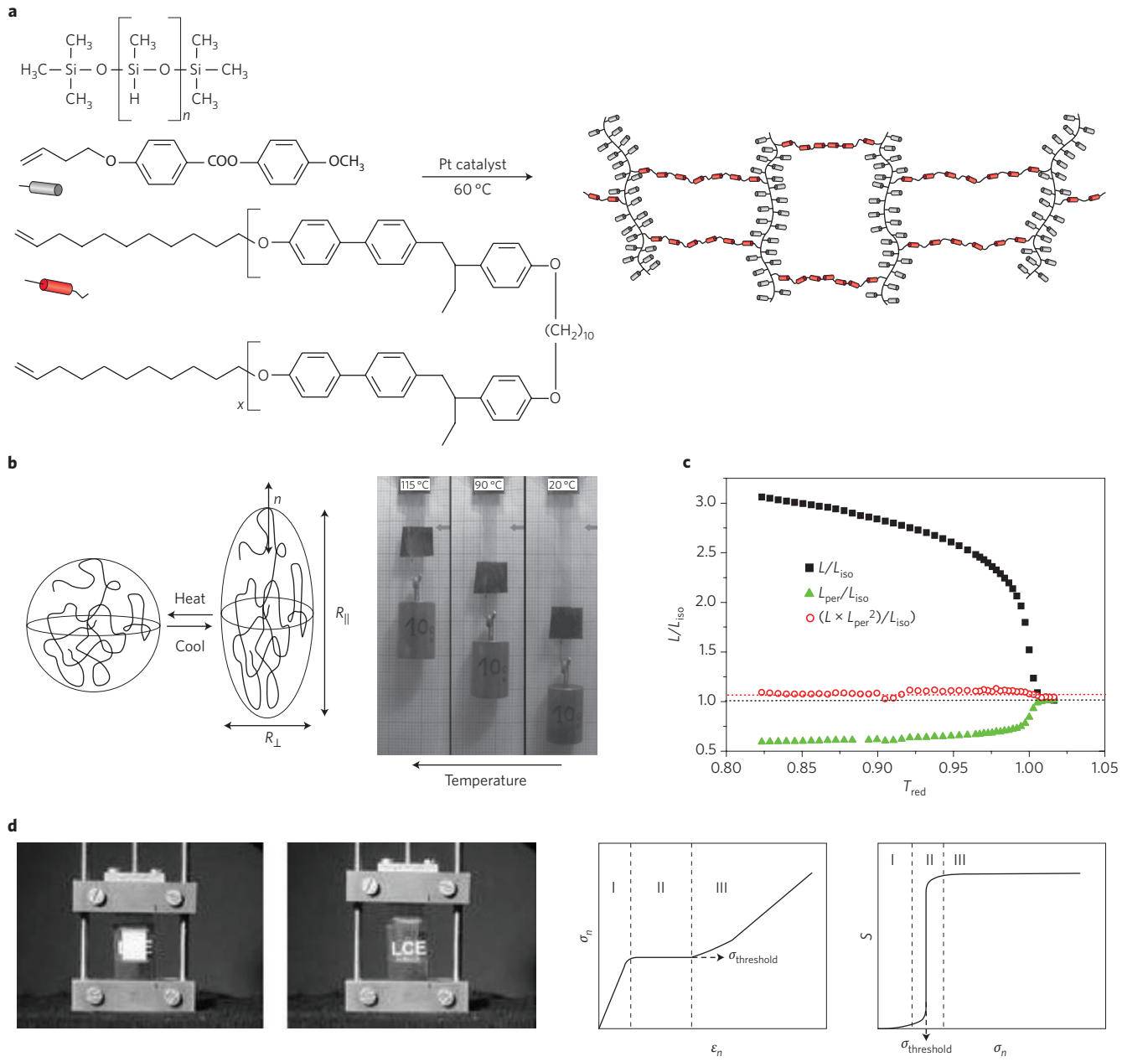

Figure 2 | Chemical composition, thermomechanical actuation and soft elasticity in liquid crystal elastomers. a, Synthesis of LCEs with polysiloxane backbone. **b**, The change in order at or above the nematic-to-isotropic phase transition results in anisotropic deformation with shrinkage of the sample parallel to the orientation direction. This is illustrated in the conversion of the average chain orientation in a unit (prolate conformation, where radii $R_{\parallel}$ is greater than $R_{\perp}$ in relation to the orientation of the nematic director, *n*) to an average chain orientation represented by a spherical conformation. Accordingly, the contractile strain can lift a 10 g weight[28]. **c**, The strain (original length, *L* divided by the length in the isotropic state, L_{iso}; L/L_{iso}) is plotted against reduced temperature (T_{red}) parallel (black squares) and perpendicular (green triangles) to the orientation direction. The relative volume, equal to $(L \times L_{per}^2)/L_{iso}$) (red circles) is constant. The large-magnitude thermomechanical responses result from thermally induced reduction in order[10] (*S*) . **d**, A polydomain LCE transitions from scattering (left) to transparent (right) as the orientation of the nematic domains align under stretching[20]. Concurrent to the optical changes, LCEs exhibit a soft-elastic plateau, evident in the stress (σ)–strain (ε) curve (region II), which deviates from classical or semi-classical elasticity (regions I and III). The changes in transparency and the soft-elastic plateaus have been related to director reorientation depicted in the plot of order (*S*) versus stress. Figure reproduced with permission from: **a**,**c**, ref. 10, © 2013 Walter De Gruyter; **b**, ref. 28, Wiley; **d**, ref. 20, Oxford Univ. Press.

The directionality of the bend of a cantilever made of a glassy LCN can be regulated by orienting the linear polarization of an ultraviolet light source to the axes of the film[81] (Fig. 4h). Because of the large concentration of azobenzene in most LCN compositions examined to date, the strong absorbance of the material localized the response to the surface, resulting in bending. Subsequent examinations of LCN materials have explored mechanical control with the intensity[82–84], polarization[81,85] and wavelength[82,83,86] of light. Oscillatory responses[87,88] have been realized in these materials as well (Fig. 4i), and the dependence of the oscillation on the exposure conditions, polarization and sample thickness has also been described[88]. Moreover, the frequency of the observed oscillation matches the expected resonant frequency of the cantilever[87]. Key to the generation of oscillatory responses is the employment of focused irradiation, which can allow the front and back surface of the cantilever to deflect into and out of the light. The contribution of photothermal

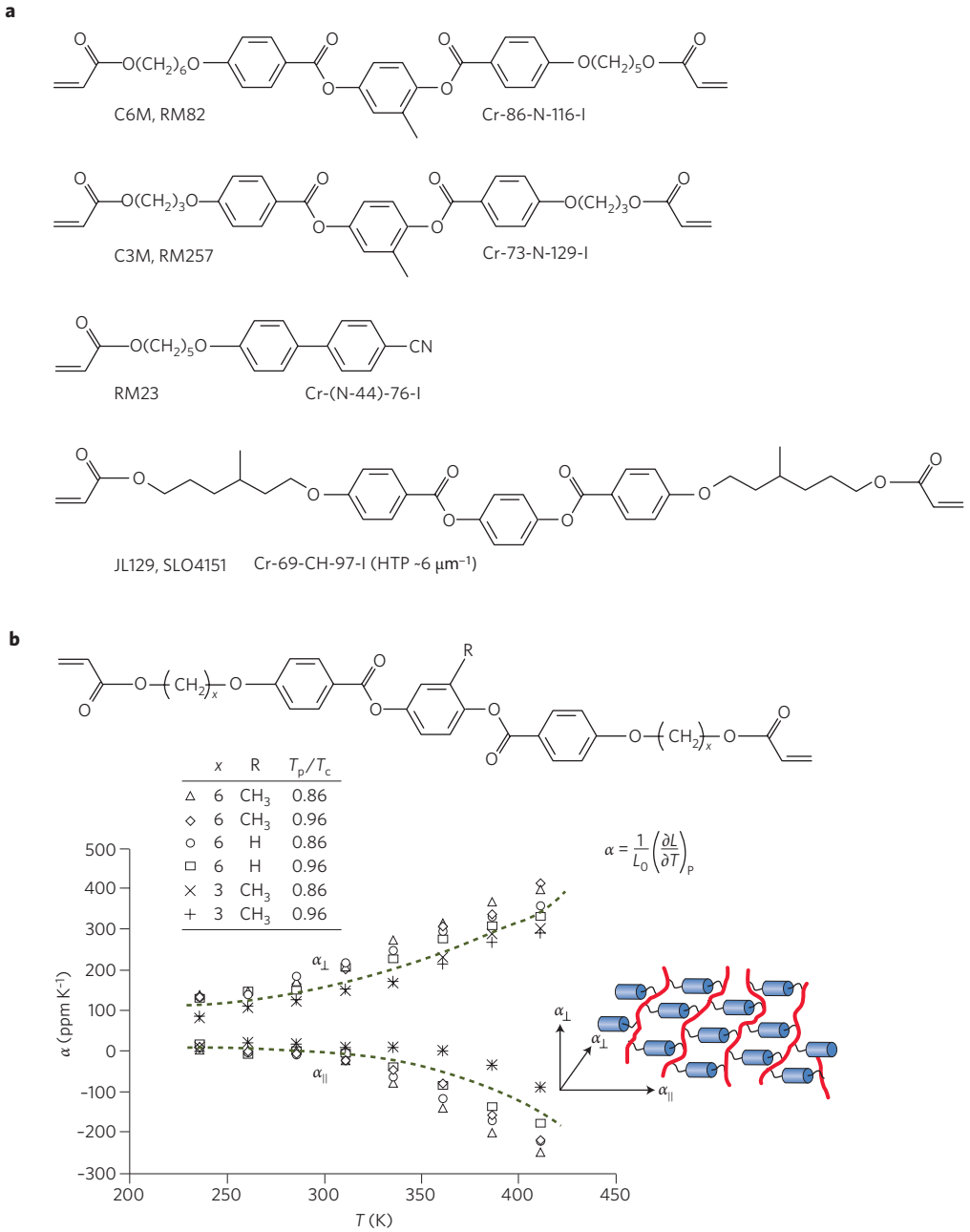

Figure 3 | Liquid crystal monomers and polymer networks. a, Chemical structures of common liquid crystal monomers. The efficiency of the chiral monomer to induce twist is referred to as helical twisting power, or HTP. Labels below the structures correspond to trade names (left) and denote phases and transition temperatures (right; Cr, crystalline; N, nematic; I, isotropic; CH, cholesteric). **b**, The thermal expansion coefficient, α, of liquid crystal networks is anisotropic in sign. The magnitude of α depends not only on the length of the aliphatic spacer unit, x, but also on the preparation conditions (polymerization temperature, T_p) and the thermotropism of the mixture (clearing temperature, T_c). The thermal expansion coefficients correspond to a series of LCNs prepared from the chemical structure shown, and with variations in the aliphatic spacer length (x) as well the presence of a methyl substituent to the mesogenic core (R). The dashed lines indicate a fit of this data. Panel **b** adapted with permission from ref. 55, Wiley.

heating was alluded to in these works, and then further clarified in subsequent studies using thermal imaging[83]. Notable recent efforts in the general area of photomechanical responses in glassy LCN materials include the preparation and photomechanical characterization of fibres[89], the inclusion of upconverting nanoparticles to allow for infrared-triggered responses[90], bidirectional actuation[85,91], shape memory[92], and the systematic examination of the role of crosslinkers on the generation of strain[86,93–95].

In addition to in-plane bending, 'flexural–torsional' (that is, bending and twisting) deflections have also been examined[81]. Polarization-controlled twisting[85], also in conditions that induce both static[83,86] and oscillatory[96] deflections, has been demonstrated as well. Yet, the magnitude of the twisting is limited in conventional domain orientations.

Taking advantage of the ability to spatially and hierarchically manipulate the orientation of anisotropy in LCN materials to generate desired effects, a five-order-of-magnitude enhancement in work generation has been achieved for azo-LCNs prepared in the planar orientation with respect to azo-LCNs prepared with hierarchical structures (such as splay or twisted nematic)[84,97]. In addition to enhancing the magnitude of planar deflections, hierarchical LCN structures also enhance the magnitude of flexural–torsional

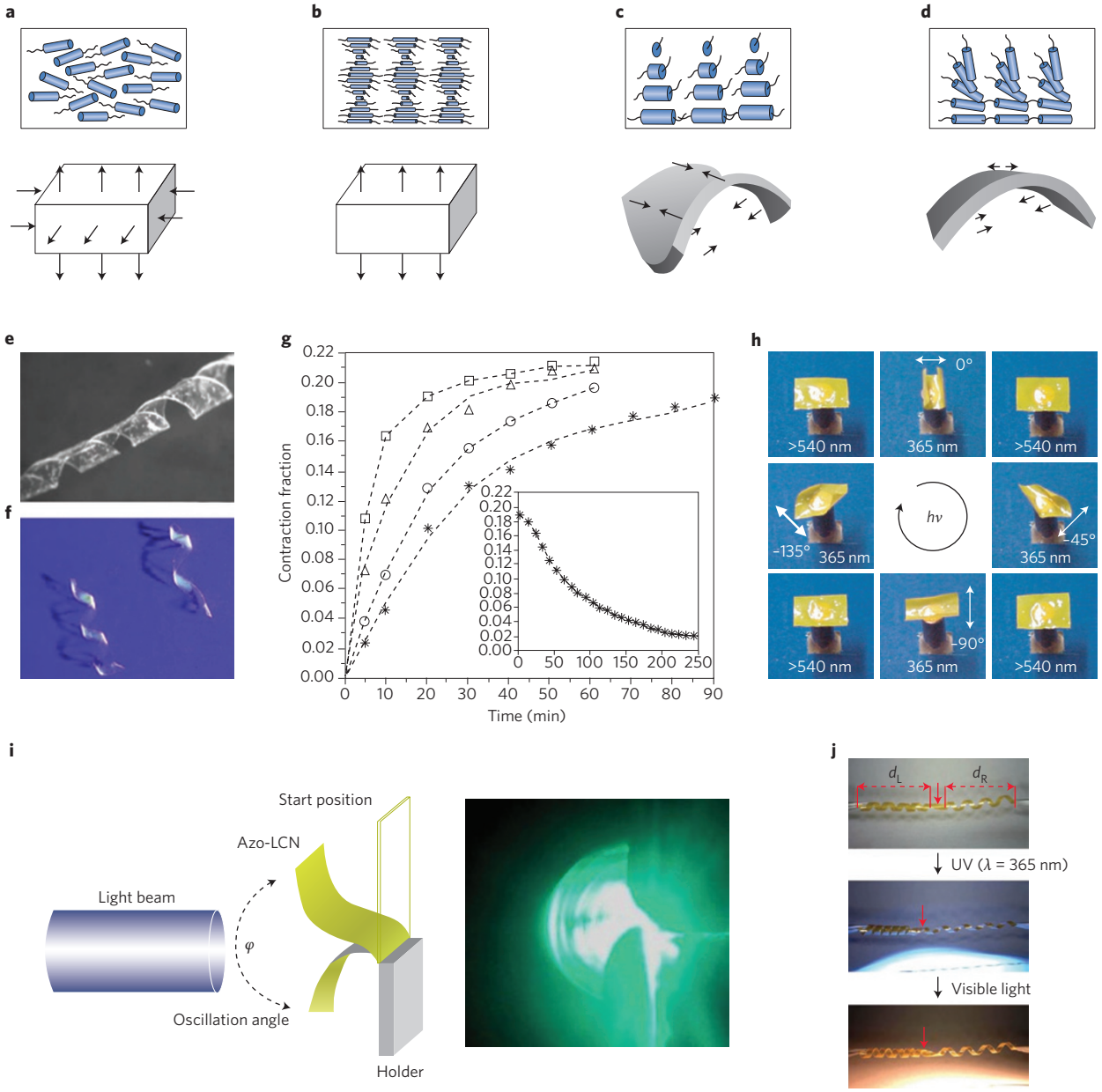

Figure 4 | Bends, twists and turns in liquid crystal polymer networks. Representation of changes in LCN or LCE dimensions on exposure to an order-disrupting stimuli. **a**–**d**, Planar uniaxial (**a**), cholesteric (**b**), twisted nematic (**c**) and splay (**d**) director profiles and their deformations corresponding to a decrease in the order parameter. **e**,**f**, Offsetting the nematic director to the principal axes of the sample can generate shear, which has been observed on heating in LCN materials. The handedness of the twisting (left or right) of the material is dictated by the material's chirality across the sample thickness. The films are approximately 6–10 mm in length and 0.5–2 mm in width. **g**, Photomechanical effects for LCEs (25 °C, asterisks; 30 °C, circles; 35 °C, triangles; 40 °C, squares) and LCNs. Inset: The relaxation of the photogenerated strain in the dark at 25 °C. **h**, Photodirected bending of a LCN film on irradiation with linearly polarized 365-nm light. The orientation of linearly polarized light (0°, −45°, −90°, −135°) dictates the directionality of the deflection of the samples. Subsequent irradiation with light of wavelength greater than 540 nm flattens the film. **i**, In appropriate optical conditions, irradiation with blue–green light can initiate oscillations[87]. The cantilever length is 5 mm. **j**, Light can also be used to introduce both left (d_L)- and right (d_R)-handed spirals in a photoresponsive LCN[99]. The films are more than 10 mm in length. Figure reproduced with permission from: **e**, ref. 58, NAS; **f**, ref. 57, Wiley; **g**, ref. 69, APS; **h**, ref. 81, Nature Publishing Group; **i**, ref. 87, RSC; **j**, ref. 99, Nature Publishing Group.

responses, as exemplified by reports of photoinduced twisting and shape formation in twisted nematic films[98,99] (Fig. 4j).

Remote heating

In addition to employing photochemistry, contactless actuation of LCN materials can be also be accomplished directly or indirectly through absorptive heating with either optical or magnetic stimuli. Distinguishing photochemical mechanisms from photothermal contributions (if any) is a consistent endeavour[86,72,73,100–104]. However, a number of recent reports intentionally hybridized photomechanical and thermomechanical effects through the addition of guest materials that are efficient heat-transfer agents. In this regard, the preparation of an LCE composed with carbon nanotube (CNT) additives initially focused on enabling electromechanical effects in these systems[105]. Building on work in non-liquid-crystalline systems[106–109], photomechanical effects in composites of CNTs and LCEs were later reported[110–117]. Although the energy transfer is indirect (that is, light to heat to work), the effects can be

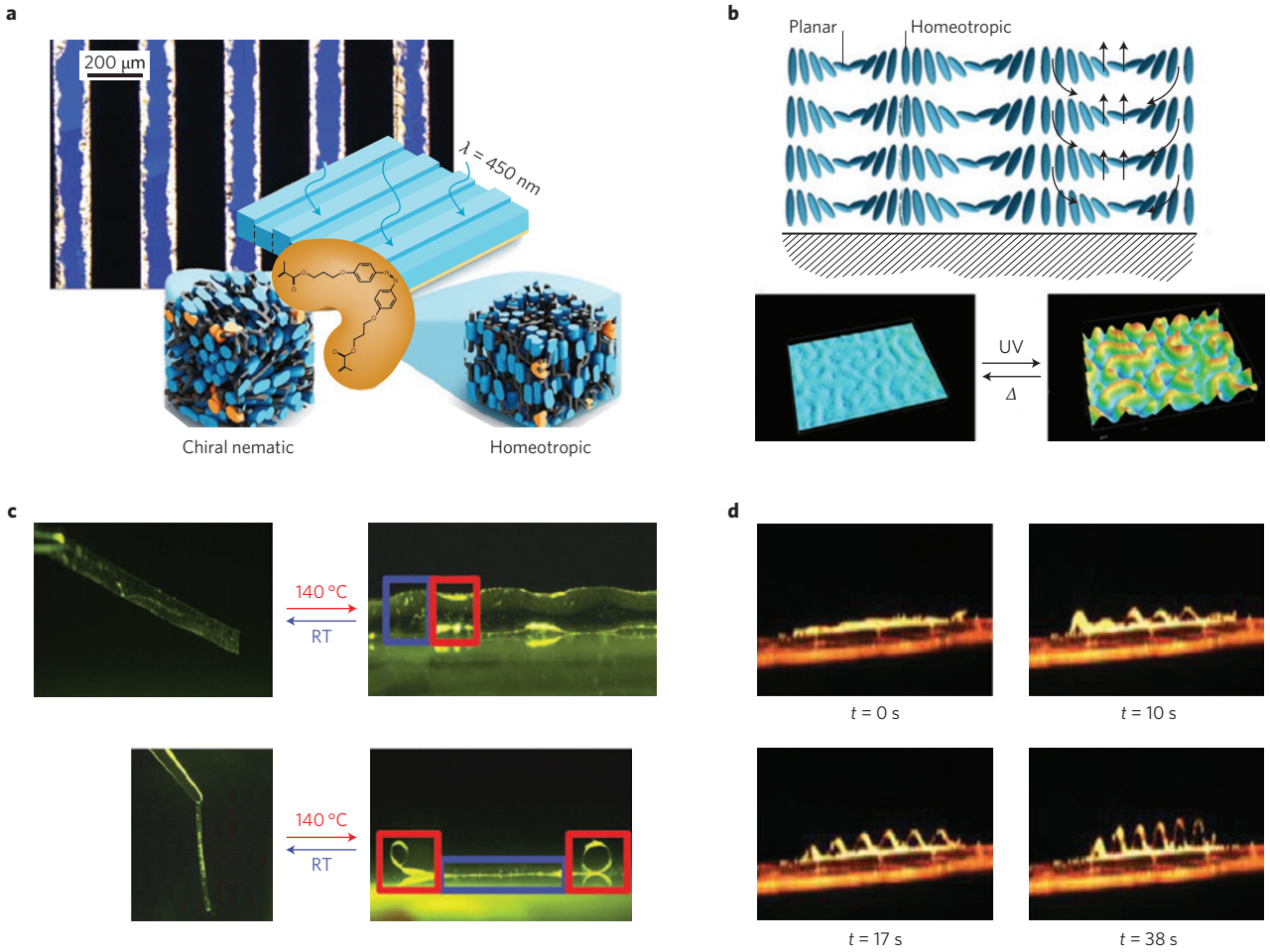

Figure 5 | Reconfigurable topography. a, Monolithic polymer coatings prepared from LCNs change topography with irradiation by light[123–125]. The polarization micrograph shows alternating stripes of a perpendicularly oriented LCN next to an area with a planar chiral-nematic order. On actuation with ultraviolet light the planar chiral areas expand, whereas the perpendicularly oriented area contracts, resulting in a regular surface profile. The process is reversible. **b**, When the axis of the helices of the chiral-nematic LCN are oriented parallel to the surface, a fingerprint pattern that switches from planar to homeotropic is formed, which when subjected to a stimulus, induces a corrugated surface roughness. **c**,**d**, Spatial variation in the local orientation of twisted nematic domains within LCN materials has been shown to generate complex mechanical responses on heating, including ripples (**c**, top right)[57], localized curling (**c**, bottom right)[57], and localized ridges (**d**)[128]. In **c**, the blue squares denote a planar nematic region and the red squares denote a twisted nematic region in the LCN films. RT, room temperature. Figure reproduced with permission from: **a**, ref. 124, Wiley; **b**, ref. 123, Wiley; **c**, ref. 57, Wiley; **d**, ref. 128, Wiley.

triggered with white light and infrared sources. The absorption of photons by CNTs or other broadband absorbers, such as graphene, is radiated as heat, and heat transfer triggers thermomechanical effects (local strain) in the polymer network. Methods to homogeneously disperse CNTs into LCEs and other matrices have been shown, and the benefits of adding CNTs, for example, increased toughness and conductivity[105,110,114,115], have also been documented. Cantilever bending has been used to visualize the response of these materials[111].

Magnetic actuation has also been harnessed in elastomeric and glassy LCNs with magnetic nanoparticles to allow for remote actuation[118–121]. For a review, see ref. 122.

Stimuli-responsive topographical effects

One of the distinguishing features of LCN materials, when compared with the large number of functional polymers developed to date, is the ability to prepare films that are homogeneous in composition but heterogeneous in mechanical response. We conclude this review of stimuli-responsive LCN materials with a summary of recent work on the programming of local anisotropy in LCN materials to yield spatially complex shape-changes or surface-variations.

LC materials can spontaneously organize, or can be forced to align. Polymerization of mixtures composed of liquid crystalline monomers has been shown to lock this complex orientation in monolithic form. This is most plainly evident in LCNs that retain the twisted nematic and splay orientations or the cholesteric LC phase (Fig. 4b–d). In each of these geometries, the director rotates across the sample thickness. Because of the association of the thermomechanical or photomechanical responses and the anisotropy of LCN materials, these geometries can be thought of as monolithic analogues to those of functionally graded composites. In combination with lateral (x–y axis) alignment techniques, such as rubbing, electric field or photoalignment, polymeric films can be prepared with domain variations across the sample thickness (z axis) so as to achieve complex topographical surface deformations[123–127].

One approach for the generation of spatially resolved variations in the order and orientation of LCNs employs the electro-optic response of materials (Fig. 3a) and electrode patterning[123–125]. The generation of topographical surface features in LCN films through this method has been recently reviewed[127]. The use of light to remotely trigger topographical features in LCN materials is illustrated in Fig. 5a,b. Using a two-step polymerization process and

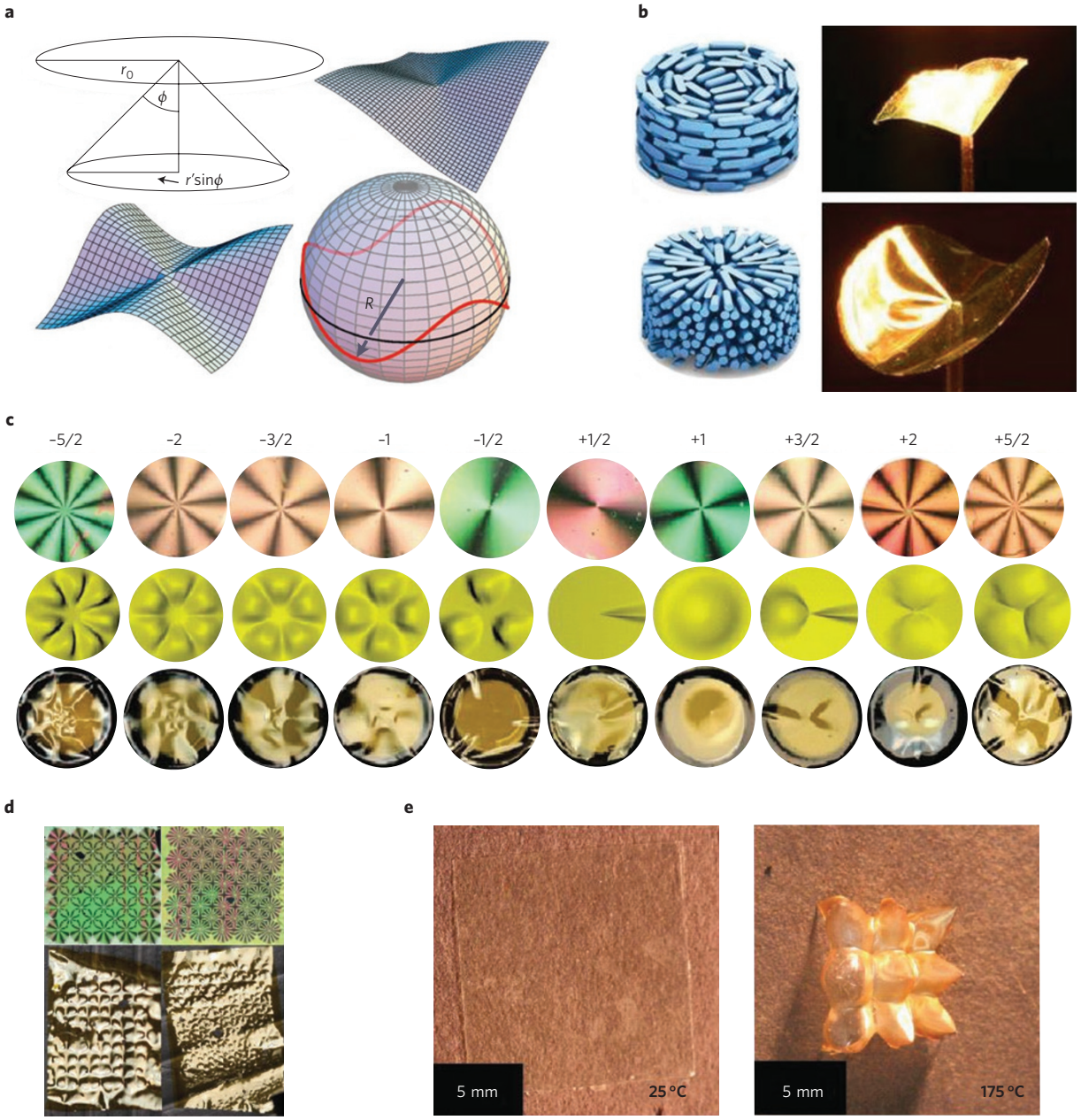

Figure 6 | Topography from topological defects. a, Theoretical examination[129] of LCNs predict conical and anticonical deformation of topologically imprinted defects of +1 strength. **b**, Schematics illustrating the nematic-director orientation of +1 radial and azimuthal defects, and experimental realization[134] of the predicted deformations in LCNs (film approximately 10 mm in diameter). **c**, Preparation and characterization of films subsumed with topological defects ranging from –5/2 to +5/2 in strength. Top row: Polarized optical micrographs confirming the charge strength as well as centre of the point singularity. Middle row: Illustration of the photoinduced mechanical response of the films on irradiation with UV light. Bottom row: Imaged photoinduced mechanical response[135]. The diameter of the films is 1 cm. **d**, Arrays of 41 +2 or +4 topological defects can be actuated to generate periodic topographical surfaces[135]. **e**, Enabled by the formulation of chemistry conducive to photoalignment techniques employed in **b**–**d**, LCE films were prepared with a 3 × 3 array of +1 radial defects[137]. The increase in strain to 60% substantially increases the deflection of the tip of the conical deformations to as much as 5 mm. Figure reproduced with permission from: **a**, ref. 129, APS; **b**, ref. 134, Wiley; **c**,**d**, ref. 135, Wiley; **e**, ref. 137, AAAS.

electric fields, the LCN material maintains alternating regions of homeotropic and planar boundary conditions. Owing to the periodic variation of the director profile in the chiral nematic regions, large surface features have been reported with heat, light and chemical stimuli. Photoalignment patterning can also be used to prepare LCN films with alternating regions of monodomain and twisted nematic orientation (Fig. 5c,d). On heating through T_g, the films exhibit complex deformation, in which the monodomain region remains flat and the twisted nematic regions ripple and curl (Fig. 5c)[57]. Patterned twisted nematic LCN materials have recently been shown to exhibit large-scale, accordion-like actuation as well[128] (Fig. 5d).

Motivated by theoretical work[129–133] (Fig. 6a), distinctive shape and surface features in LCN films with topological defects have been achieved. In an initial demonstration (Fig. 6b), LCN films containing a heat-transfer dye were prepared with central-point defects of charge +1/2, +1, −1/2 and −1, as well as combinations thereof[134]. Defects (Fig. 6c) and arrays of defects (Fig. 6d) with strengths ranging from ±0.5 to 10 have demonstrated rich and diversified photoinduced topographical features[135].

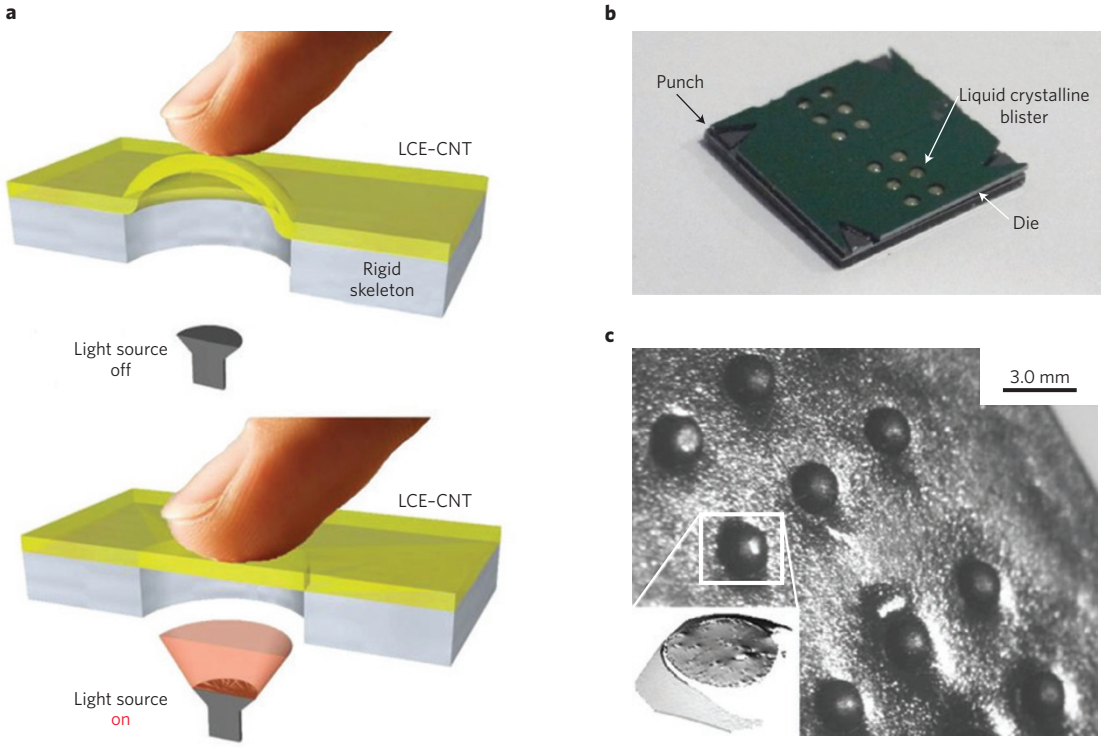

Figure 7 | Communicating through touch. Haptic-display principle based on the selective actuation of an elastomeric LCN prepared with carbon nanotube (CNT) additives[148]. **a**, The elastomeric LCN contracts when a light source switches on, leading to a flat surface. **b**,**c**, Preparation of the perforations by stretching the LCE–CNT composite across a die and punching it to generate blisters illustrated in **a** and depicted in **c**. In **c**, Perforations apparent in the blisters (inset) could be used in applications, such as a dynamic Braille display. Figure reproduced with permission: **a**,**b**, ref. 148, IOP.

Recent efforts have extended preparation methods to programme LCEs[136]. Very recently, LCE materials were prepared in cells that are sensitive to photoalignment[137], and very large conical deformations were shown to be capable of generating as much as 2.5 J kg^{-1} in work (Fig. 6e)[137]. Furthermore, the ability to spatially pattern (voxelate) local regions of the material was employed to prepare a self-folding Miura-ori origami pattern[137].

Outlook

To project the future opportunities for stimuli-responsive LCNs and LCEs, it is important to distinguish the materials' novel features with respect to the broader literature on stimuli-responsive materials and on active mechanisms in conventional materials and actuators. Compared with peer material technologies, such as shape-memory polymers, electroactive polymers and other responsive materials, stimuli-responsive LCNs and LCEs have many similarities as well as some advantages and disadvantages. For instance, both LCNs and LCEs are capable of exhibiting either shape-fixing (shape memory)[43–45,57,92,138–141] or shape-restoring (artificial muscle)[10,23–25,37–39] responses. Within the larger stimuli-responsive polymeric literature, both of these properties have been identified as potential enablers to the realization of novel biomedical devices, soft robotics and morphing structures. The ability of LCNs or LCEs to self-organize to form materials of homogeneous composition with spatial variation of the mechanical response (evident in the localization of planar or hierarchical domain orientations in Fig. 5c,d, or topological defect structures in Fig. 6a–e) is not simple to emulate in other stimuli-responsive materials. Key to enabling the distinctive ability to generate spatial variation in the directionality and hierarchical orientation in LCN materials are surface-alignment methods, which can involve rubbing, magnetic fields and light (photoalignment). Magnetic-field alignment has recently been used to prepare a dynamic aperture[142]. Photoalignment methods offer the potential for elaborate spatial control to form volume elements (voxels), analogous to the pixelation of LC displays[137]. The generation of shape-changes or dynamic topographical features has potential uses in microfluidics[143,144], flow control[144], solar-energy harvesting[87,145–147] and haptic displays[112–114,148,149] (Fig. 7).

Many reports to date have discussed the potential use of these materials in actuation. Yet it is critical to define what is meant by actuation. Sometimes actuation is meant to simply imply motion. Others define an actuator as a system in which the stimuli-responsive element is but a small part of a larger system composed of amplifying elements and other mechanisms. Regardless of the definition, the term actuation implies purpose. One significant challenge is the extension of the basic understanding of the chemistry and physics of these materials, and their responses to stimuli, to what and how these can enable distinctive performance when in the hands of a mechanical designer. Towards this end, it is important for individuals in the community to engage and partner with peers in mechanics to frame and articulate potential end uses that will ultimately guide the materials development and characterization processes. In this respect, an excellent resource is the Ashby plots[150].

Stimuli-responsive liquid-crystalline polymer networks offer a promising means to generate useful functional devices. As detailed in this Review, a diverse range of responses have already been reported with a number of stimuli. Building on the foundational knowledge of the response of these films, future work exploiting the ability to pattern the director profile of these materials to generate engineered materials without creases or interconnections shows promise in a range of applications in haptic displays, lab-on-chip, aerospace and optics.

Received 24 July 2014; accepted 26 August 2015; published online 22 October 2015

References

1. Reinitzer, F. *Beiträge zur kenntniss des cholesterins. Monatsh. Chem.* **9,** 421–441 (1888).
2. Collings, P. J. & Hird, M. *An Introduction to Liquid Crystals: Chemistry and Physics* (CRC Press, 1997).
3. Prasad, S. K. Photostimulated and photosuppressed phase transitions in liquid crystals. *Angew. Chem. Int. Ed.* **51,** 10708–10710 (2012).
4. Schmidt-Mende, L. *et al.* Self-organized discotic liquid crystals for high-efficiency organic photovoltaics. *Science* **293,** 1119–1122 (2001).
5. Verbunt, P. P. C. *et al.* Increased efficiency of luminescent solar concentrators after application of organic wavelength selective mirrors. *Opt. Express* **20,** A655–A668 (2012).
6. Li, Q. *Liquid Crystals Beyond Displays: Chemistry, Physics, and Applications* (John Wiley & Sons, 2012).
7. Broer, D. J., Crawford, G. P. & Zumer, S. *Cross-Linked Liquid Crystalline Systems: From Rigid Polymer Networks to Elastomers* (CRC Press, 2011).
8. Woltman, S. J., Jay, G. D. & Crawford, G. P. Liquid-crystal materials find a new order in biomedical applications. *Nature Mater.* **6,** 929–938 (2007).
9. Beyer, P., Terentjev, E. M. & Zentel, R. Monodomain liquid crystal main chain elastomers by photocrosslinking. *Macromol. Rapid Commun.* **28,** 1485–1490 (2007).
10. Wermter, H. & Finkelmann, H. Liquid crystalline elastomers as artificial muscles. *e-Polymers* **1,** 111–123 (2001).
11. Urayama, K. Selected issues in liquid crystal elastomers and gels. *Macromolecules* **40,** 2277–2288 (2007).
12. Urayama, K., Honda, S. & Takigawa, T. Electrically driven deformations of nematic gels. *Phys. Rev. E* **71,** 051713 (2005).
13. Urayama, K., Honda, S. & Takigawa, T. Deformation coupled to director rotation in swollen nematic elastomers under electric fields. *Macromolecules* **39,** 1943–1949 (2006).
14. Vorlander, D. Investigation of the molecular form by means of crystalline liquids. *Z. Phys. Chem.* **105,** 211–254 (1923).
15. Jackson, W. J. & Kuhfuss, H. F. Liquid crystal polymers. I. Preparation and properties of *p*-hydroxybenzoic acid copolyesters. *J. Polym. Sci. Polym. Chem.* **14,** 2043–2058 (1976).
16. Finkelmann, H., Kock, H-J. & Rehage, G. Investigations on liquid crystalline polysiloxanes. 3. Liquid crystalline elastomers — a new type of liquid crystalline material. *Macromol. Rapid Commun.* **2,** 317–322 (1981).
17. Portugall, M., Ringsdorf, H. & Zentel, R. Synthesis and phase behavior of liquid crystalline polyacrylates. *Makromol. Chem.* **183,** 2311–2321 (1982).
18. Ringsdorf, H. & Zentel, R. Liquid crystalline side chain polymers and their behavior in the electric field. *Makromol. Chem.* **183,** 1245–1256 (1982).
19. Küpfer, J. & Finkelmann, H. Nematic liquid single crystal elastomers. *Makromol. Chem. Rapid Commun.* **12,** 717–726 (1991).
20. Terentjev, E. M. & Warner, M. *Liquid Crystal Elastomers* (Oxford Univ. Press, 2009).
21. Warner, M., Bladon, P. & Terentjev, E. "Soft elasticity" — deformation without resistance in liquid crystal elastomers. *J. Phys. II* **4,** 93–102 (1994).
22. De Gennes, P. G. *Possibilites offertes par la reticulation de polymeres en presence d'un cristal liquide. Phys. Lett.* **28A,** 725–726 (1969).
23. Li, M-H., Keller, P., Li, B., Wang, X. & Brunet, M. Light-driven side-on nematic elastomer actuators. *Adv. Mater.* **15,** 569–572 (2003).
24. Buguin, A., Li, M-H., Silberzan, P., Ladoux, B. & Keller, P. Micro-actuators: when artificial muscles made of nematic liquid crystal elastomers meet soft lithography. *J. Am. Chem. Soc.* **128,** 1088–1089 (2006).
25. Li, M-H. & Keller, P. Artificial muscles based on liquid crystal elastomers. *Phil. Trans. R. Soc. A* **364,** 2763–2777 (2006).
26. Tajbakhsh, A. R. & Terentjev, E. M. Spontaneous thermal expansion of nematic elastomers. *Eur. Phys. J. E* **6,** 181–188 (2001).
27. Finkelmann, H., Kim, S. T., Muñoz, A., Palffy-Muhoray, P. & Taheri, B. Tunable mirrorless lasing in cholesteric liquid crystalline elastomers. *Adv. Mater.* **13,** 1069–1072 (2001).
28. Ohm, C., Brehmer, M. & Zentel, R. Liquid crystalline elastomers as actuators and sensors. *Adv. Mater.* **22,** 3366–3387 (2010).
29. Broer, D. J., Boven, J., Mol, G. N. & Challa, G. *In-situ* photopolymerization of oriented liquid-crystalline acrylates. 3. Oriented polymer networks from a mesogenic diacrylate. *Makromol. Chem.* **190,** 2255–2268 (1989).
30. Broer, D. J., Finkelmann, H. & Kondo, K. *In-situ* photopolymerization of an oriented liquid-crystalline acrylate. *Makromol. Chem.* **189,** 185–194 (1988).
31. Broer, D. J., Hikmet, R. A. M. & Challa, G. *In-situ* photopolymerization of oriented liquid-crystalline acrylates. 4. Influence of a lateral methyl substituent on monomer and oriented polymer network properties of a mesogenic diacrylate. *Makromol. Chem.* **190,** 3201–3215 (1989).
32. Broer, D. J., Mol, G. N. & Challa, G. *In situ* photopolymerization of an oriented liquid-crystalline acrylate. 2. *Makromol. Chem.* **190,** 19–30 (1989).
33. De Gennes, P. G. in *Polymer Liquid Crystals* (eds Cifferi, A. *et al.*) 115–131 (Academic, 1982).
34. Cotton, J. P. & Hardouin, F. Chain conformation of liquid-crystalline polymers studied by small-angle neutron scattering. *Prog. Polym. Sci.* **22,** 795–828 (1997).
35. De Gennes, P. G. *Réflexions sur un type de polymères nématiques. C. R. Acad. Sci.* **B281,** 101–103 (1975).
36. Urayama, K., Kohmon, E., Kojima, M. & Takigawa, T. Polydomain–monodomain transition of randomly disordered nematic elastomers with different cross-linking histories. *Macromolecules* **42,** 4084–4089 (2009).
37. De Gennes, P. G., Hebert, M. & Kant, R. Artificial muscles based on nematic gels. *Macromol. Symp.* **113,** 39–49 (1997).
38. Hebert, M., Kant, R. & De Gennes, P. G. Dynamics and thermodynamics of artificial muscles based on nematic gels. *J. Phys. I* **7,** 909–919 (1997).
39. Thomsen, D. L. III. *et al.* Liquid crystal elastomers with mechanical properties of a muscle. *Macromolecules* **34,** 5868–5875 (2001).
40. de Jeu, W. H. *Liquid Crystal Elastomers: Materials and Applications* (Springer, 2012).
41. Fleischmann, E-K., Ohm, C., Serra, C. & Zentel, R. Preparation of soft microactuators in a continuous flow synthesis using a liquid-crystalline polymer crosslinker. *Macromol. Chem. Phys.* **213,** 1871–1878 (2012).
42. Evans, J. S. *et al.* Active shape-morphing elastomeric colloids in short-pitch cholesteric liquid crystals. *Phys. Rev. Lett.* **110,** 187802 (2013).
43. Rousseau, I. A. & Mather, P. T. Shape memory effect exhibited by smectic-C liquid crystalline elastomers. *J. Am. Chem. Soc.* **125,** 15300–15301 (2003).
44. Burke, K. A. & Mather, P. T. Soft shape memory in main-chain liquid crystalline elastomers. *J. Mater. Chem.* **20,** 3449–3457 (2010).
45. Burke, K. A. & Mather, P. T. Evolution of microstructure during shape memory cycling of a main-chain liquid crystalline elastomer. *Polymer* **54,** 2808–2820 (2013).
46. Zupancic, B., Zalar, B., Remskar, M. & Domenici, V. Actuation of gold-coated liquid crystal elastomers. *Appl. Phys. Express* **6,** 021701 (2013).
47. Wu, Z. L. *et al.* Microstructured nematic liquid crystalline elastomer surfaces with switchable wetting properties. *Adv. Funct. Mater.* **23,** 3070–3076 (2013).
48. Wei, R., He, Y., Wang, X. & Keller, P. Nematic liquid crystalline elastomer grating and microwire fabricated by micro-molding in capillaries. *Macromol. Rapid Commun.* **34,** 330–334 (2013).
49. Corbett, D. R. & Adams, J. M. Tack energy and switchable adhesion of liquid crystal elastomers. *Soft Matter* **9,** 1151–1163 (2013).
50. Hikmet, R. A. M. & Broer, D. J. Dynamic mechanical properties of anisotropic networks formed by liquid-crystalline acrylates. *Polymer* **32,** 1627–1632 (1991).
51. Broer, D. J., Mol, G. N. & Challa, G. *In-situ* photopolymerization of oriented liquid-crystalline acrylates. 5. Influence of the alkylene spacer on the properties of the mesogenic monomers and the formation and properties of oriented polymer networks. *Makromol. Chem.* **192,** 59–74 (1991).
52. Broer, D. J. & Mol, G. N. Anisotropic thermal expansion of densely crosslinked oriented polymer networks. *Polym. Eng. Sci.* **31,** 625–631 (1991).
53. Hikmet, R. A. M., Zwerver, B. H. & Broer, D. J. Anisotropic polymerization shrinkage behavior of liquid-crystalline diacrylates. *Polymer* **33,** 89–95 (1992).
54. Wie, J. J., Lee, K. M., Ware, T. H. & White, T. J. Twists and turns in glassy, liquid crystalline polymer networks. *Macromolecules* **48,** 1087–1092 (2015).
55. Mol, G. N., Harris, K. D., Bastiaansen, C. W. M. & Broer, D. J. Thermo-mechanical responses of liquid-crystal networks with a splayed molecular organization. *Adv. Funct. Mater.* **15,** 1155–1159 (2005).
56. Harris, K. D., Bastiaansen, C. W. M., Lub, J. & Broer, D. J. Self-assembled polymer films for controlled agent-driven motion. *Nano Lett.* **5,** 1857–1860 (2005).
57. Lee, K. M., Bunning, T. J. & White, T. J. Autonomous, hands-free shape memory in glassy, liquid crystalline polymer networks. *Adv. Mater.* **24,** 2839–2843 (2012).
58. Sawa, Y. *et al.* Shape selection of twist-nematic-elastomer ribbons. *Proc. Natl Acad. Sci. USA* **108,** 6364–6368 (2011).
59. Sawa, Y. *et al.* Shape and chirality transitions in off-axis twist nematic elastomer ribbons. *Phys. Rev. E* **88,** 022502 (2013).
60. Ohm, C. *et al.* Preparation of actuating fibers of oriented main-chain liquid crystalline elastomers by a wet spinning process. *Soft Matter* **7,** 3730–3734 (2011).
61. Ikeda, T. & Zhao, Y. *Smart Light-Responsive Materials: Azobenzene-Containing Polymers and Liquid Crystals* (Wiley, 2009).
62. Corbett, D. & Warner, M. Changing liquid crystal elastomer ordering with light — a route to opto-mechanically responsive materials. *Liq. Cryst.* **36,** 1263–1280 (2009).
63. Ikeda, T., Mamiya, J-I. & Yu, Y. Photomechanics of liquid-crystalline elastomers and other polymers. *Angew. Chem. Int. Ed.* **46,** 506–528 (2007).
64. Ikeda, T. & Ube, T. Photomobile polymer materials: from nano to macro. *Mater. Today* **14,** 480–487 (October, 2011).

65. Koerner, H., White, T. J., Tabiryan, N. V., Bunning, T. J. & Vaia, R. A. Photogenerating work from polymers. *Mater. Today* **11,** 34–42 (July–August, 2008).
66. White, T. J. Light to work transduction and shape memory in glassy, photoresponsive macromolecular systems: trends and opportunities. *J. Polym. Sci. B* **50,** 877–880 (2012).
67. Eisenbach, C. D. Isomerization of aromatic azo chromophores in poly(ethyl acrylate) networks and photomechanical effect. *Polymer* **21,** 1175–1179 (1980).
68. Agolini, F. & Gay, F. P. Synthesis and properties of azoaromatic polymers. *Macromolecules* **3,** 349–351 (1970).
69. Finkelmann, H., Nishikawa, E., Pereira, G. G. & Warner, M. A new opto-mechanical effect in solids. *Phys. Rev. Lett.* **87,** 015501 (2001).
70. Sanchez-Ferrer, A., Merekalov, A. & Finkelmann, H. Opto-mechanical effect in photoactive nematic side-chain liquid-crystalline elastomers. *Macromol. Rapid Commun.* **32,** 671–678 (2011).
71. Camacho-Lopez, M., Finkelmann, H., Palffy-Muhoray, P. & Shelley, M. Fast liquid crystal elastomer swims in the dark. *Nature Mater.* **3,** 307–310 (2004).
72. Cviklinski, J., Tajbakhsh, A. R. & Terentjev, E. M. UV isomerisation in nematic elastomers as a route to photo-mechanical transducer. *Eur. Phys. J. E* **9,** 427–434 (2002).
73. Hogan, P. M., Tajbakhsh, A. R. & Terentjev, E. M. UV manipulation of order and macroscopic shape in nematic elastomers. *Phys. Rev. E* **65,** 041720 (2002).
74. Warner, M. & Mahadevan, L. Photoinduced deformations of beams, plates, and films. *Phys. Rev. Lett.* **92,** 134302 (2004).
75. Corbett, D. & Warner, M. Nonlinear photoresponse of disordered elastomers. *Phys. Rev. Lett.* **96,** 237802 (2006).
76. Corbett, D. & Warner, M. Linear and nonlinear photoinduced deformations of cantilevers. *Phys. Rev. Lett.* **99,** 174302 (2007).
77. Corbett, D. & Warner, M. Bleaching and stimulated recovery of dyes and of photocantilevers. *Phys. Rev. E* **77,** 051710 (2008).
78. Corbett, D. & Warner, M. Polarization dependence of optically driven polydomain elastomer mechanics. *Phys. Rev. E* **78,** 061701 (2008).
79. Nath, N. K., Panda, M. K., Sahoo, S. C. & Naumov, P. Thermally induced and photoinduced mechanical effects in molecular single crystals — a revival. *CrystEngComm* **16,** 1850–1858 (2014).
80. Kim, T., Zhu, L., Al-Kaysi, R. O. & Bardeen, C. J. Organic photomechanical materials. *ChemPhysChem* **15,** 400–414 (2014).
81. Yu, Y., Nakano, M. & Ikeda, T. Photomechanics: directed bending of a polymer film by light. *Nature* **425,** 145 (2003).
82. Yamada, M. *et al.* Photomobile polymer materials: towards light-driven plastic motors. *Angew. Chem. Int. Ed.* **47,** 4986–4988 (2008).
83. Lee, K. M. & White, T. J. Photochemical mechanism and photothermal considerations in the mechanical response of monodomain, azobenzene-functionalized liquid crystal polymer networks. *Macromolecules* **45,** 7163–7170 (2012).
84. Harris, K. D. *et al.* Large amplitude light-induced motion in high elastic modulus polymer actuators. *J. Mater. Chem.* **15,** 5043–5048 (2005).
85. Tabiryan, N., Serak, S., Dai, X-M. & Bunning, T. Polymer film with optically controlled form and actuation. *Opt. Express* **13,** 7442–7448 (2005).
86. Lee, K. M., Tabiryan, N. V., Bunning, T. J. & White, T. J. Photomechanical mechanism and structure–property considerations in the generation of photomechanical work in glassy, azobenzene liquid crystal polymer networks. *J. Mater. Chem.* **22,** 691–698 (2012).
87. Serak, S., Tabiryan, N., White, T. J., Vaia, R. A. & Bunning, T. J. Liquid crystalline polymer cantilever oscillators fueled by light. *Soft Matter* **6,** 779–783 (2010).
88. White, T. J. *et al.* High frequency photodriven polymer oscillator. *Soft Matter* **4,** 1796–1798 (2008).
89. Yoshino, T. *et al.* Three-dimensional photomobility of crosslinked azobenzene liquid-crystalline polymer fibers. *Adv. Mater.* **22,** 1361–1363 (2010).
90. Wu, W. *et al.* NIR-light-induced deformation of cross-linked liquid-crystal polymers using upconversion nanophosphors. *J. Am. Chem. Soc.* **133,** 15810–15813 (2011).
91. White, T. J., Serak, S. V., Tabiryan, N. V., Vaia, R. A. & Bunning, T. J. Polarization-controlled, photodriven bending in monodomain liquid crystal elastomer cantilevers. *J. Mater. Chem.* **19,** 1080–1085 (2009).
92. Lee, K. M., Koerner, H., Vaia, R. A., Bunning, T. J. & White, T. J. Light-activated shape memory of glassy azobenzene liquid crystal polymer networks. *Soft Matter* **7,** 4318–4324 (2011).
93. Mamiya, J-i., Yoshitake, A., Kondo, M., Yu, Y. & Ikeda, T. Is chemical crosslinking necessary for the photoinduced bending of polymer films? *J. Mater. Chem.* **18,** 63–65 (2008).
94. Kondo, M. *et al.* Effect of concentration of photoactive chromophores on photomechanical properties of crosslinked azobenzene liquid-crystalline polymers. *J. Mater. Chem.* **20,** 117–122 (2010).
95. Lee, K. M., Koerner, H., Vaia, R. A., Bunning, T. J. & White, T. J. Relationship between the photomechanical response and the thermomechanical properties of azobenzene liquid crystalline polymer networks. *Macromolecules* **43,** 8185–8190 (2010).
96. Lee, K. M. *et al.* Photodriven, flexural-torsional oscillations of glassy azobenzene liquid crystal polymer networks. *Adv. Funct. Mater.* **15,** 2913–2918 (2011).
97. van Oosten, C. L., Harris, K. D., Bastiaansen, C. W. M. & Broer, D. J. Glassy photomechanical liquid-crystal network actuators for microscale devices. *Eur. Phys. J. E* **23,** 329–336 (2007).
98. Wie, J. J., Lee, K. M., Smith, M. L., Vaia, R. A. & White, T. J. Torsional mechanical responses in azobenzene functionalized liquid crystalline polymer networks. *Soft Matter* **9,** 9303–9310 (2013).
99. Iamsaard, S. *et al.* Conversion of light into macroscopic helical motion. *Nature Chem.* **6,** 229–235 (2014).
100. Warner, M. & Terentjev, E. Thermal and photo-actuation in nematic elastomers. *Macromol. Symp.* **200,** 81–92 (2003).
101. Harvey, C. L. M. & Terentjev, E. M. Role of polarization and alignment in photoactuation of nematic elastomers. *Eur. Phys. J. E* **23,** 185–189 (2007).
102. Hon, K. K., Corbett, D. & Terentjev, E. M. Thermal diffusion and bending kinetics in nematic elastomer cantilever. *Eur. Phys. J. E* **25,** 83–89 (2008).
103. Dawson, N. J., Kuzyk, M. G., Neal, J., Luchette, P. & Palffy-Muhoray, P. Modeling the mechanisms of the photomechanical response of a nematic liquid crystal elastomer. *J. Opt. Soc. Am. B* **28,** 2134–2141 (2011).
104. Dawson, N. J., Kuzyk, M. G., Neal, J., Luchette, P. & Palffy-Muhoray, P. Experimental studies of the mechanisms of photomechanical effects in a nematic liquid crystal elastomer. *J. Opt. Soc. Am. B* **28,** 1916–1921 (2011).
105. Courty, S., Mine, J., Tajbakhsh, A. R. & Terentjev, E. M. Nematic elastomers with aligned carbon nanotubes: new electromechanical actuators. *Europhys. Lett.* **64,** 654–660 (2003).
106. Koerner, H., Price, G., Pearce, N. A., Alexander, M. & Vaia, R. A. Remotely actuated polymer nanocomposites — stress-recovery of carbon-nanotube-filled thermoplastic elastomers. *Nature Mater.* **3,** 115–120 (2004).
107. Ahir, S. V. & Terentjev, E. M. Photomechanical actuation in polymer–nanotube composites. *Nature Mater.* **4,** 491–495 (2005).
108. Ahir, S. V. & Terentjev, E. M. Fast relaxation of carbon nanotubes in polymer composite actuators. *Phys. Rev. Lett.* **96,** 133902 (2006).
109. Ahir, S. V., Squires, A. M., Tajbakhsh, A. R. & Terentjev, E. M. Infrared actuation in aligned polymer–nanotube composites. *Phys. Rev. B* **73,** 085420 (2006).
110. Marshall, J. E., Ji, Y., Torras, N., Zinoviev, K. & Terentjev, E. M. Carbon-nanotube sensitized nematic elastomer composites for IR-visible photo-actuation. *Soft Matter* **8,** 1570–1574 (2012).
111. Torras, N., Zinoviev, K. E., Marshall, J. E., Terentjev, E. M. & Esteve, J. Bending kinetics of a photo-actuating nematic elastomer cantilever. *Appl. Phys. Lett.* **99,** 254102 (2011).
112. Campo, E. M. *et al.* Nano opto-mechanical systems (NOMS) as a proposal for tactile displays. *Proc. SPIE* **8107,** 81070H (2011).
113. Camargo, C. J. *et al.* Microstamped opto-mechanical actuator for tactile displays. *Proc. SPIE* **8107,** 810709 (2011).
114. Camargo, C. J. *et al.* Localised actuation in composites containing carbon nanotubes and liquid crystalline elastomers. *Macromol. Rapid Commun.* **32,** 1953–1959 (2011).
115. Ji, Y., Huang, Y. Y., Rungsawang, R. & Terentjev, E. M. Dispersion and alignment of carbon nanotubes in liquid crystalline polymers and elastomers. *Adv. Mater.* **22,** 3436–3440 (2010).
116. Li, C., Liu, Y., Lo, C-w. & Jiang, H. Reversible white-light actuation of carbon nanotube incorporated liquid crystalline elastomer nanocomposites. *Soft Matter* **7,** 7511–7516 (2011).
117. Yang, L., Setyowati, K., Li, A., Gong, S. & Chen, J. Reversible infrared actuation of carbon nanotube-liquid crystalline elastomer nanocomposites. *Adv. Mater.* **20,** 2271–2275 (2008).
118. Kaiser, A., Winkler, M., Krause, S., Finkelmann, H. & Schmidt, A. M. Magnetoactive liquid crystal elastomer nanocomposites. *J. Mater. Chem.* **19,** 538–543 (2009).
119. Winkler, M., Kaiser, A., Krause, S., Finkelmann, H. & Schmidt, A. M. Liquid crystal elastomers with magnetic actuation. *Macromol. Symp.* **291–292,** 186–192 (2010).
120. Zhou, Y. *et al.* Hierarchically structured free-standing hydrogels with liquid crystalline domains and magnetic nanoparticles as dual physical cross-linkers. *J. Am. Chem. Soc.* **134,** 1630–1641 (2012).
121. Petsch, S. *et al.* A thermotropic liquid crystal elastomer micro-actuator with integrated deformable micro-heater. *IEEE 27th Int. Conf. Micro Electro Mechanical Sys.* 905–908 (2014).
122. Chambers, M. *et al.* Liquid crystal elastomer–nanoparticle systems for actuation. *J. Mater. Chem.* **19,** 1524–1531 (2009).
123. Liu, D. & Broer, D. J. Self-assembled dynamic 3D fingerprints in liquid-crystal coatings towards controllable friction and adhesion. *Angew. Chem. Int. Ed.* **53,** 4542–4546 (2014).

124. Liu, D., Bastiaansen, C. W. M., den Toonder, J. M. J. & Broer, D. J. Photo-switchable surface topologies in chiral nematic coatings. *Angew. Chem. Int. Ed.* **51,** 892–896 (2012).
125. Liu, D., Bastiaansen, C. W. M., den Toonder, J. M. J. & Broer, D. J. (Photo-) thermally induced formation of dynamic surface topographies in polymer hydrogel networks. *Langmuir* **29,** 5622–5629 (2013).
126. Stumpel, J. E., Broer, D. J. & Schenning, A. P. H. J. Stimuli-responsive photonic polymer coatings. *Chem. Commun.* **50,** 15839–15848 (2014).
127. Liu, D. & Broer, D. J. Liquid crystal polymer networks: preparation, properties, and applications of films with patterned molecular alignment. *Langmuir* **30,** 13499–13509 (2014).
128. de Haan, L. T. *et al.* Accordion-like actuators of multiple 3D patterned liquid crystal polymer films. *Adv. Funct. Mater.* **24,** 1251–1258 (2014).
129. Modes, C. D., Bhattacharya, K. & Warner, M. Disclination-mediated thermo-optical response in nematic glass sheets. *Phys. Rev. E* **81,** 060701 (2010).
130. Modes, C. D. & Warner, M. Blueprinting nematic glass: systematically constructing and combining active points of curvature for emergent morphology. *Phys. Rev. E* **84,** 021711 (2011).
131. Modes, C. D. & Warner, M. Responsive nematic solid shells: topology, compatibility, and shape. *EPL* **97,** 36007 (2012).
132. Modes, C. D. & Warner, M. The activated morphology of grain boundaries in nematic solid sheets. *Proc. SPIE* **8279,** 82790Q (2012).
133. Modes, C. D., Warner, M., Sanchez-Somolinos, C., de Haan, L. T. & Broer, D. Mechanical frustration and spontaneous polygonal folding in active nematic sheets. *Phys. Rev. E* **86,** 060701 (2013).
134. de Haan, L. T., Sanchez-Somolinos, C., Bastiaansen, C. M. W., Schenning, A. P. H. J. & Broer, D. J. Engineering of complex order and the macroscopic deformation of liquid crystal polymer networks. *Angew. Chem. Int. Ed.* **51,** 12469–12472 (2012).
135. McConney, M. E. *et al.* Topography from topology: photoinduced surface features generated in liquid crystal polymer networks. *Adv. Mater.* **25,** 5880–5885 (2013).
136. Pei, Z. *et al.* Mouldable liquid-crystalline elastomer actuators with exchangeable covalent bonds. *Nature Mater.* **13,** 36–41 (2014).
137. Ware, T. H., McConney, M. E., Wie, J. J., Tondiglia, V. P. & White, T. J. Voxelated liquid crystal elastomers. *Science* **347,** 982–984 (2015).
138. Yang, Z., Huck, W. T. S., Clarke, S. M., Tajbakhsh, A. R. & Terentjev, E. M. Shape-memory nanoparticles from inherently non-spherical polymer colloids. *Nature Mater.* **4,** 486–490 (2005).
139. Ahir, S. V., Tajbakhsh, A. R. & Terentjev, E. M. Self-assembled shape-memory fibers of triblock liquid-crystal polymers. *Adv. Funct. Mater.* **16,** 556–560 (2006).
140. Qin, H. & Mather, P. T. Combined one-way and two-way shape memory in a glass-forming nematic network. *Macromolecules* **42,** 273–280 (2009).
141. Ahn, S-k. & Kasi, R. M. Exploiting microphase-separated morphologies of side-chain liquid crystalline polymer networks for triple shape memory properties. *Adv. Funct. Mater.* **21,** 4543–4549 (2011).
142. Schuhladen, S. *et al.* Iris-like tunable aperture employing liquid-crystal elastomers. *Adv. Mater.* **26,** 7247–7251 (2014).
143. Chen, M. *et al.* Photodeformable CLCP material: study on photo-activated microvalve applications. *Appl. Phys. A* **102,** 667–672 (2011).
144. van Oosten, C. L., Bastiaansen, C. W. M. & Broer, D. J. Printed artificial cilia from liquid-crystal network actuators modularly driven by light. *Nature Mater.* **8,** 677–682 (2009).
145. Hiscock, T., Warner, M. & Palffy-Muhoray, P. Solar to electrical conversion via liquid crystal elastomers. *J. Appl. Phys.* **109,** 104506 (2011).
146. Li, C., Liu, Y., Huang, X. & Jiang, H. Direct sun-driven artificial heliotropism for solar energy harvesting based on a photo-thermomechanical liquid-crystal elastomer nanocomposite. *Adv. Funct. Mater.* **22,** 5166–5174 (2012).
147. Yin, R. *et al.* Can sunlight drive the photoinduced bending of polymer films? *J. Mater. Chem.* **19,** 3141–3143 (2009).
148. Camargo, C. J. *et al.* Batch fabrication of optical actuators using nanotube-elastomer composites towards refreshable Braille displays. *J. Micromech. Microeng.* **22,** 075009 (2012).
149. Torras, N. *et al.* Tactile device based on opto-mechanical actuation of liquid crystal elastomers. *Sensor. Actuat. A* **208,** 104–112 (2014).
150. Zupan, M., Ashby, M. F. & Fleck, N. A. Actuator classification and selection — the development of a database. *Adv. Eng. Mater.* **4,** 933–940 (2002).

Acknowledgements

T.J.W. acknowledges the support of the Air Force Office of Scientific Research and of the Materials and Manufacturing Directorate of the Air Force Research Laboratory.

Additional information

Reprints and permissions information is available online at www.nature.com/reprints. Correspondence and requests for materials should be addressed to T.J.W and D.J.B.

Competing financial interests

The authors declare no competing financial interests.